molecules

MDPI

Article

Synthesis and Characterization of Phosphinecarboxamide and Phosphinecarbothioamide, and Their Complexation with Palladium(II) Complex †

Masumi Itazaki [1,2,*], Kento Okabayashi [2], Takanari Matsutani [2], Tomoya Nochida [2], Toshiyuki Moriuchi [1,2] and Hiroshi Nakazawa [1,2,*]

[1] Department of Chemistry, Graduate School of Science, Osaka Metropolitan University, Sumiyoshi-ku, Osaka 558-8585, Japan
[2] Department of Chemistry, Graduate School of Science, Osaka City University, Sumiyoshi-ku, Osaka 558-8585, Japan
* Correspondence: mitazaki@omu.ac.jp (M.I.); nakazawa@omu.ac.jp (H.N.); Tel.: +81-6-6605-3123 (M.I.); +81-6-6605-2547 (H.N.)
† This paper is dedicated to Professor Koop Lammertsma to celebrate his 2021 Arbuzov Prize.

Abstract: Reactions of isocyanates/isothiocyanates with primary and secondary phosphines without solvent at room temperature afforded phosphinecarboxamide/phosphinecarbothioamide, respectively, in excellent yields. Furthermore, palladium complex $Pd(COD)Cl_2$ was allowed to react with $Ph_2PC(O)NHPh$ (**1a**) to afford $[Pd\{Ph_2PC(O)NHPh\text{-}\kappa P\}_2Cl_2]$ (**3**). On the other hand, the reaction of $Pd(COD)Cl_2$ with 1 eq. of $Ph_2PC(S)NHPh$ (**2a**) afforded $[PdCl_2\{Ph_2PC(S)NHPh\text{-}\kappa P,S\}]$ (**4**). In the case of a 1:2 molar ratio, $[PdCl\{Ph_2PC(S)NHPh\text{-}\kappa P,S\}\{Ph_2PC(S)NHPh\text{-}\kappa P\}]Cl$ (**5**) was formed. The newly obtained compounds were fully characterized using multielement NMR measurements and elemental analyses. In addition, the molecular structures of $Ph_2PC(O)NH(CH_2)_2Cl$ (**1j**), $Ph_2PC(S)NHPh(4\text{-}Cl)$ (**2c**), and **3**–**5** were determined using single-crystal X-ray diffraction.

Keywords: hydrophosphination; phosphinecarboxamide; phosphinecarbothioamide; palladium(II) complex; hydrogen bond; *cis/trans* isomerization; crystal structure

check for updates

Citation: Itazaki, M.; Okabayashi, K.; Matsutani, T.; Nochida, T.; Moriuchi, T.; Nakazawa, H. Synthesis and Characterization of Phosphinecarboxamide and Phosphinecarbothioamide, and Their Complexation with Palladium(II) Complex. *Molecules* **2022**, *27*, 5564. https://doi.org/10.3390/molecules27175564

Academic Editor: Prasad V. Bharatam

Received: 1 August 2022
Accepted: 23 August 2022
Published: 29 August 2022

1. Introduction

Phosphinecarboxamides $R_2PC(O)NR'_2$ and phosphinecarbothioamides $R_2PC(S)NR'_2$ are phosphorus-analogs of urea and thiourea, and these are interesting compounds in coordination chemistry because of the variety of coordination modes. These compounds are known to act as a *P*-coordinated monodentate ligand (type I) [1–7], a *P,S*-coordinated bidentate ligand forming a four-membered chelate ring (type II for phosphinecarbothioamide) [8–13], and a bridging ligand for two metal centers (type III and type IV for phosphinecarbothioamide) [7,14] (Figure 1).

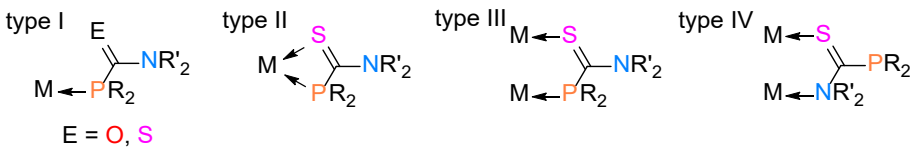

Figure 1. Typical coordination modes for phosphinecarboxamide and phosphinecarbothioamide.

One of the most efficient methods for the synthesis of phosphinecarboxamide/phosphinecarbothioamide is the hydrophosphination of isocyanates/isothiocyanates. The reaction without a metal catalyst has some drawbacks (low yield and long reaction time) [15]. Therefore, metal-mediated methods have been developed, and there have been two reports on rare earth metals (La, Y, Eu, Er, Yb) [16,17], two reports on Th and

U [18,19], one report on Fe [20] and one on Zn [21] for both isocyanates and isothiocyanates, and one report each on Zr [22], Cu [23] and Sb [24] for isocyanates to date. However, the removal of toxic metals after the end of the reaction is required when a metal compound is used. Therefore, the development of metal-free methods has been researched.

Recently, the transition-metal complex bearing 1,1′-bis(diphenylphosphinecarboxamidyl) ferrocene $Fc(NHC(O)PPh_2)_2$ as a ligand has been reported to exhibit unique properties. The tetranuclear Pt complex with six $Fc(NHC(O)PPh_2)_2$ has a hollow cage structure [25], and the macrocyclic dimer of $Fc(NHC(O)PPh_2\text{-}AuCl)_2$, induced by aurophilic interactions, shows helical chirality induction into the ferrocene core when using chiral proline methyl ester hydrochloride [26]. Although phosphinecarboxamide has attracted attention as a ligand, no examples have been reported comparing the ligand behavior of phosphinecarboxamide and its thiocarbonyl analog (phosphinecarbothioamides) with the same transition-metal complex precursor. In this study, we report the synthesis of isocyanate/isothiocyanate without using a transition-metal catalyst and the reactions of $Pd(COD)Cl_2$ (COD = η^2:η^2-1,5-cyclooctadiene) being a typical Pd(II) complex with $Ph_2PC(E)NHPh$ (E = O, S). We found the first example of the thermal *cis*/*trans* isomerization of a transition-metal complex with phosphinecarboxamide and phosphinecarbothioamide having intra- and/or inter-molecular hydrogen bonds. A part of this work was preliminarily reported in [27].

2. Results and Discussion

2.1. Synthesis of Phosphinecarboxamide and Phosphinecarbothioamide

Previously, we found that iron catalyzes the hydrophosphination of the unsaturated C–C bonds of alkynes and vinylphosphines with secondary phosphines [28,29]. In these reactions, phosphine compounds do not act as a catalyst poison. Therefore, we thought that the hydrophosphination reaction of isocyanates and isothiocyanates may be adaptable in our system. We performed the reaction-condition screening of the hydrophosphination of phenylisocyanates and found that no solvent was the key reaction condition. The desired hydrophosphination product, $Ph_2PC(O)NHPh$ **1a**, was obtained within 30 min in >99% yield at room temperature when catalyst and solvent were not used Scheme 1.

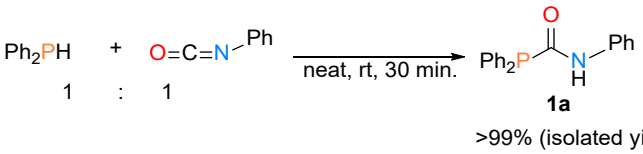

Scheme 1. Hydrophosphination reaction of phenylisocyanate with diphenylphosphine.

We examined the substrate scope and limitation for the hydrophosphination of isocyanates with diphenylphosphine (Scheme 2). Phenylisocyanates with an electron-withdrawing group such as F, Cl, Br, and CF_3 at the *para* position and Cl at the *meta* position on the phenyl ring were readily converted (within 40 min) into the corresponding phosphinecarboxamides in excellent yields (**1b**, **1c**, **1d**, **1e**, **1h**). The reaction of *para*-methoxyphenylisocyanate and that of 1-naphthylisocyanate took longer (**1f**, **1g**). Isocyanates with aliphatic substituent were also adaptable to this reaction (**1i** and **1j**). When 2-chlorophenylisocyanate, sterically bulky cyclohexylisocyanate, and 1-adamantylisocyanate were used, the desired products were not yielded. The double hydrophosphination of 1,3- and 1,4-diisocyanatobenzene were found to yield the desired products, **1k** and **1l**, in 85% and 92% yields, respectively. In addition, the triple hydrophosphination product **1m** could be obtained in 64% yield.

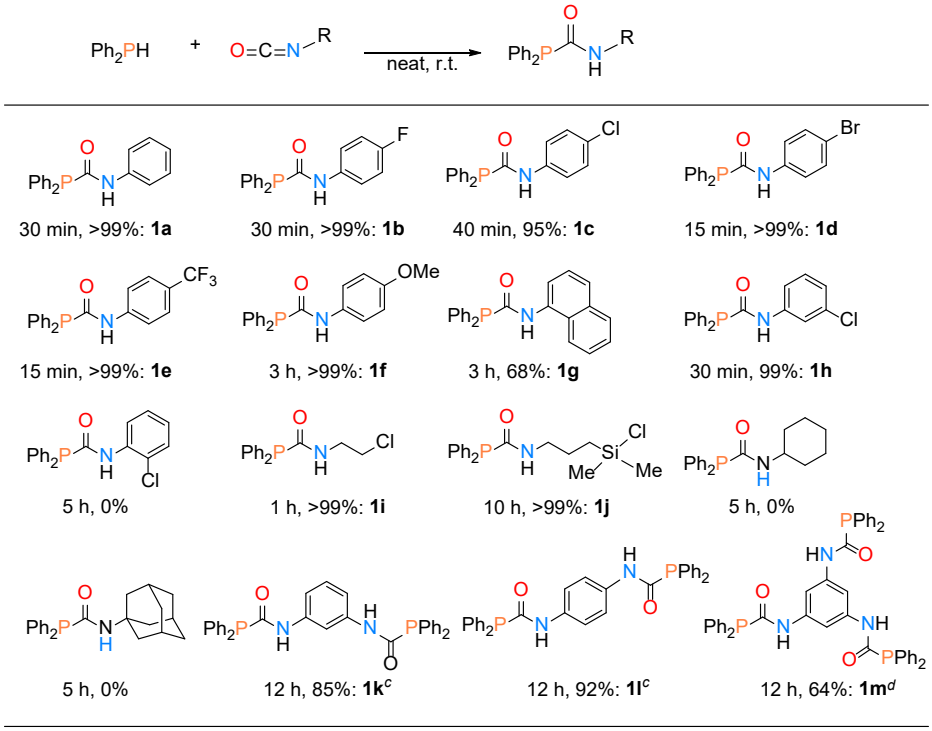

Scheme 2. Scope and limitation for hydrophosphination of isocyanates with diphenylphosphine [a,b]. [a] Ph_2PH: isocyanate = 1:1 molar ratio. [b] Isolated yield. [c] 80 °C, 2 equiv. of Ph_2PH was used (vs. isocyanate). [d] 80 °C, 3 equiv. of Ph_2PH was used (vs. isocyanate).

The results of the scope and limitation for the hydrophosphination of phenylisocyanate with phosphine compounds are summarized in Scheme 3. Diphenylphosphine analogs with electron-donating or -withdrawing groups such as Me, OMe, and F at the *para* position of the phenyl rings, and dialkylphosphines such as $^{t}Bu_2PH$ and $^{i}Pr_2PH$ were also adaptable to this reaction. In the case of primary phosphine $PhPH_2$, single hydrophosphination product **1s** was obtained in 71%, but a long reaction time (3 days) was required because of the small amount of hexane existing in commercially available $PhPH_2$ (see Section 3.1).

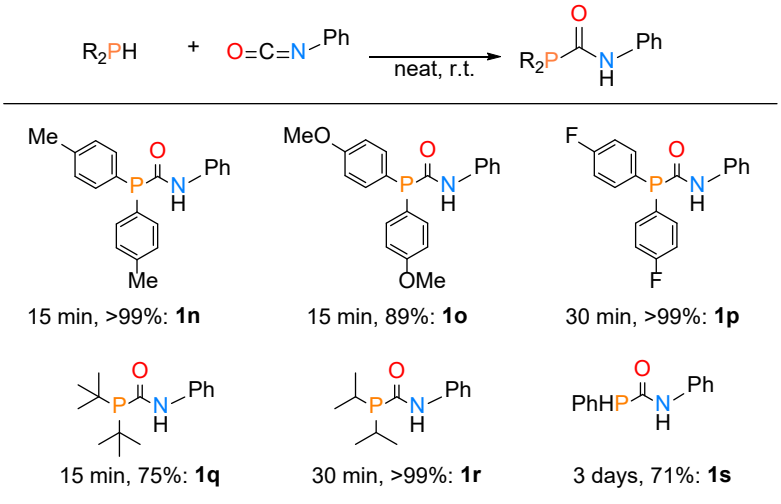

Scheme 3. Hydrophosphination of phenylisocyanate with secondary phosphines R_2PH and primary phosphine $PhPH_2$ [a,b]. [a] Phosphine compound: isocyanate = 1:1 molar ratio. [b] Isolated yield.

We reported the hydrophosphination of phenylisothiocyanate with diphenylphosphine to give the corresponding phosphinecarbothioamide **2a** in a previous study [27]. Very recently, the hydrophosphination of isothiocyanates using a catalyst-free method was reported by Zhu and Wang's group [30]. For comparison, we also examined the synthesis of phosphinecarbothioamide without catalyst and solvent. Scheme 4 summarizes the results showing good functional group tolerance. Several isothiocyanates could be employed in the reaction, in which R is the phenyl ring with withdrawing groups such as F, Cl, Br, and CF_3 at the *para* position (**2a**, **2b**, **2c**, **2d**, **2e**). These reactions were completed within 30 min. Using 4-methoxyphenylisothiocyanate, 1-naphthylisothiocyanate and 3-chlorophenylisocyanate, a long reaction time was required (**2f**, **2g**, **2h**). Surprisingly, the hydrophosphination reaction of 2-chlorophenylisothiocyanate took place. This result is in contrast with the hydrophosphination of 2-chlorophenylisocyanate. Isothiocyanate with an aliphatic substituent was also adaptable to this reaction (**2j**). 1-Adamathylisothiocyanate did not react. These tendencies are similar to those observed for the corresponding isocyanates except for 2-chlorophenylisocyanate. The hydrophosphination of phenylisothiocyanate with $(4\text{-methylphenyl})_2PH$ also proceeded well (**2k**).

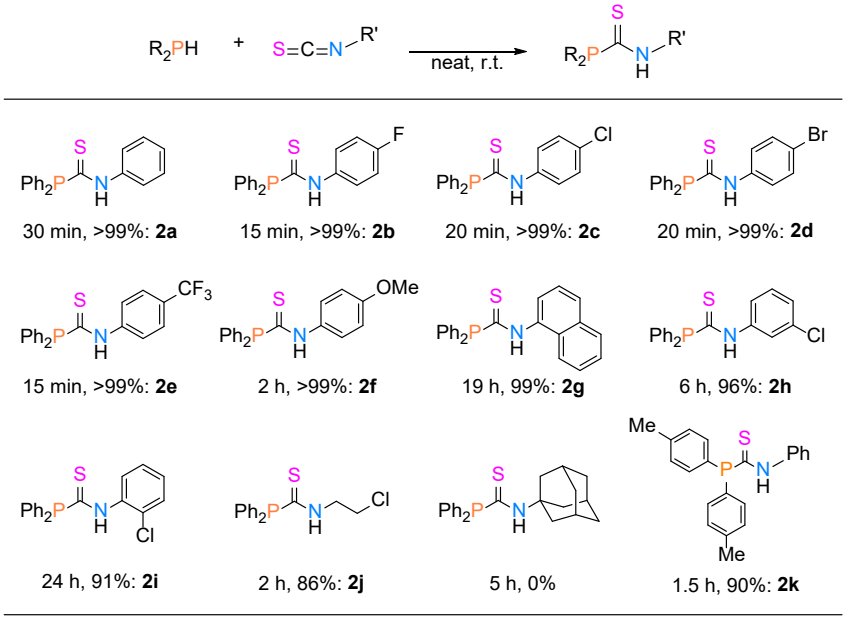

Scheme 4. Scope and limitation for the hydrophosphination of isothiocyanates with diarylphosphine [a,b]. [a] Phosphine compound: isothiocyanate = 1:1 molar ratio. [b] Isolated yield.

The molecular structures of **1i** and **2c** were determined using a single-crystal X-ray diffraction study. Two independent molecules of **1i** were crystallized in the unsymmetric unit. The ORTEP drawings are shown in Figure 2a) for **1i** (P1 molecule) and b) for **2c**, along with selected bond lengths and angles. The bond distances of P1–C3 (1.870(2) Å) and C3–N1 (1.328(3) Å) for **1i** were similar to those of P1–C7 (1.8541(17) Å) and N1–C7 (1.336(2) Å) for **2c**. The phosphinecarboxamide and phosphinecarbothioamide moieties displayed a pyramidalized geometry at the P atom (sum of angle around P1 = 330.8° for **1i** and 306.5° for **2c**), indicating that the π-electron conjugation of the C=O and C=S did not extend to the P. In contrast, the planar carboxamide and carbothioamide moieties (sum of angle around N1 = 359.9° for **1i** and 360.0° for **2c**) were observed, showing the delocalization of π-electron density between the carbonyl (thiocarbonyl) and amide groups. These were consistent with the previously reported phosphinecarboxamide [31].

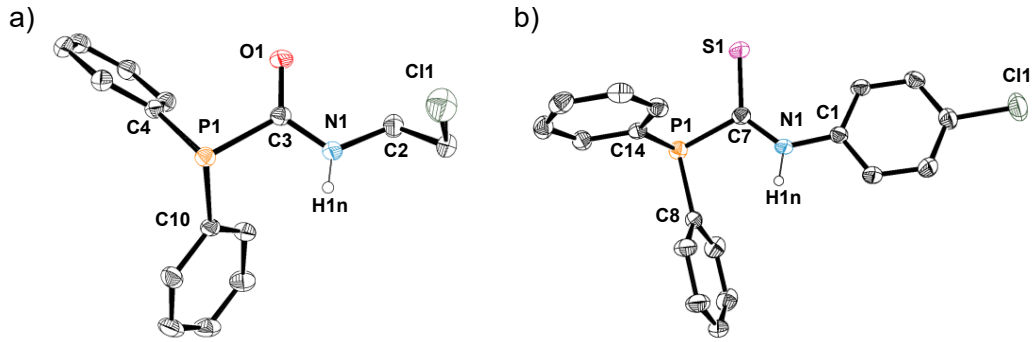

Figure 2. ORTEP drawings of (**a**) **1i** (P1 molecule) and (**b**) **2c** with thermal ellipsoids at 50% probability. Hydrogen atoms (except for NH protons) are omitted for simplicity. Selected bond lengths (Å) and angles (°): P1–C3 1.870(2), N1–C2 1.452(3), N1–C3 1.328(3), C3–O1 1.231(2), N1–H1n 0.81(3), C3–P1–C4 98.62(9), C3–P1–C10 103.32(9), C4–P1–C10 101.86(9), C2–N1–C3 123.30(19), C2–N1–H1n 121.1(19), C3–N1–H1n 115.4(19) for **1i** (P1 molecule); P1–C7 1.8541(17), N1–C1 1.420(2), N1–C7 1.336(2), C7–S1 1.6540(18), N1–H1n 0.86(2), C7–P1–C14 101.63(8), C7–P1–C8 102.88(7), C8–P1–C14 101.95(7), C1–N1–C7 132.20(16), C1–N1–H1n 110.5(13), C7–N1–H1n 117.3(13) for **2c**.

It is noteworthy that gram-scale practical reactions were successfully performed: phosphinecarboxamide **1a** and phosphinecarbothioamide **2a** were isolated in 90% and 99% yields, respectively (Scheme 5).

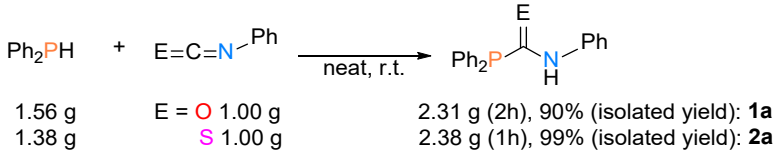

Scheme 5. Gram-scale synthesis of phosphinecarboxamide and phosphinecarbothioamide.

2.2. Synthesis of Palladium(II) Complexes with Phosphinecarboxamide and Phosphinecarbothioamide

The reaction of $Pd(COD)Cl_2$ with **1a** at a 1:2 molar ratio produced the related bis(phosphinecarboxamide)palladium complex [Pd{$Ph_2PC(O)NHPh$-κ*P*}$_2Cl_2$] (**3**) in 97% yield. Complex **3** was obtained even when $Pd(COD)Cl_2$ was treated with 1 equiv. of **1a** (NMR yield: 48%) (Scheme 6). The NH proton signal of **1a** was not observed in $CDCl_3$ because of the overlapped phenyl protons, but it was observed at δ 7.13 ppm in C_6D_6 [20]. In the ^{1}H NMR spectrum of **3** in $CDCl_3$, the NH proton was observed at δ 10.56 ppm. This chemical shift indicates that the NH of **3** is involved in hydrogen bonding. The ^{31}P NMR spectrum of **3** showed two singlets (δ 25.5 ppm and 32.5 ppm in ca. 8:1 ratio) at 20 °C. The ratio of the two singlets depended on the temperature (ca. 16:1 at 50 °C and ca. 4:1 at −50 °C) (see Supplementary Materials, Figure S1). We think that this Pd complex adopts a planar geometry and performs *cis/trans* isomerization; the signal of δ 25.5 ppm was assigned to *trans*-**3** and that of δ 32.5 ppm to *cis*-**3**. The thermal *cis/trans* isomerization of bis(phosphine)palladium(II) complex is well known [32,33]. In our system, the thermodynamic parameters $\Delta H°$ (1.3×10^4 Jmol^{-1}) and $\Delta S°$ (6.2×10^1 JK^{-1} mol^{-1}) of **3** were obtained using van't Hoff plots (see Supplementary Materials, Figure S2). These values were similar to those in the previous report [32,33].

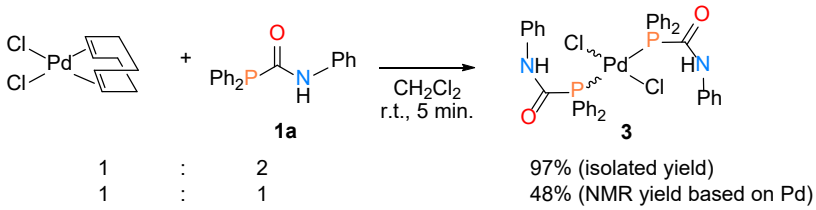

Scheme 6. Reactions of $Pd(COD)Cl_2$ with $Ph_2PC(O)NHPh$ **1a**.

Since single crystals were obtained from the reaction solution of Scheme 6, an X-ray structure analysis was performed, and the ORTEP drawing was obtained, as depicted in Figure 3, with the atomic numbering scheme. The complex (*trans*-**3**) was confirmed to adopt a typical square-planar configuration; the palladium center had two Cl atoms and two *P*-coordinated $Ph_2PC(O)NHPh$ (**1a**), which were *trans*-positioned with respect to each other. This molecule had two N–H···Cl intramolecular hydrogen bonds (Cl1···H2n (2.28(4) Å), Cl2···H1n (2.22(6) Å)). The hydrogen bonds in addition to the bulkiness of **1a** were considered to be the reason for the *trans* geometry. This is the first example of a planar complex in which two phosphinecarboxamide ligands are coordinated to the *trans* position. The Pd–P bond distances (2.3574(9), 2.3707(9) Å) were longer than those of previously reported for *cis*-$[PdCl_2\{(\pm)\text{-pbap}\}_2]$ (pbap = 3-phenyl-1,3-dihydrobenzo [1,3]azaphosphol-2-one) (2.2420(7), 2.2282(7) Å) [2]. The sum of the angles around N1 and N2 atoms were ca. 360°. These angles were similar to those previously reported [31]. This observation indicates that the delocalization of π-electron density between the carbonyl and amide groups was maintained even after complex formation.

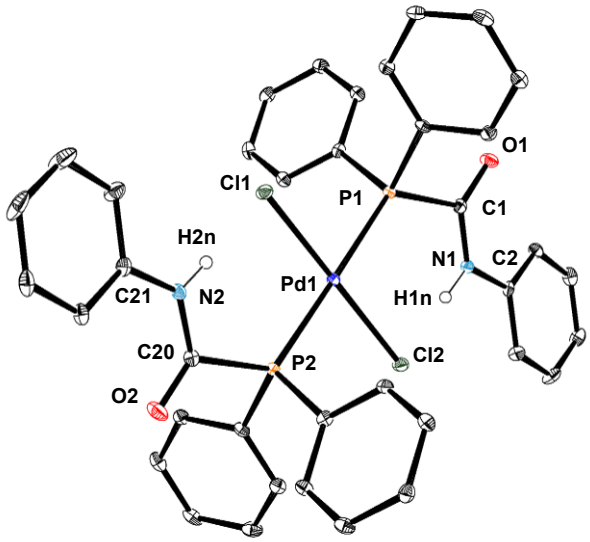

Figure 3. ORTEP drawing of *trans*-**3** with thermal ellipsoids at 30% probability. Hydrogen atoms (except for NH protons) are omitted for simplicity. Selected bond lengths (Å) and angles (°): Pd1–P1 2.3707(9), Pd1–P2 2.3574(9), Pd1–Cl1 2.3033(10), Pd1–Cl2 2.3132(10), C1–O1 1.218(4), C20–O2 1.218(4), N1–H1n 0.92(6), N2–H2n 0.83(4), P1–Pd1–P2 178.99(5), P1–Pd1–Cl1 82.33(4), P1–Pd1–Cl2 98.14(4), P2–Pd1–Cl1 96.70(4), P2–Pd1–Cl2 82.83(4), Cl1–Pd1–Cl2 179.29(4).

The reaction of $Pd(COD)Cl_2$ with $Ph_2PC(S)NHPh$ (**2a**) at a 1:1 molar ratio produced $[PdCl_2\{Ph_2PC(S)NHPh\text{-}\kappa P,S\}]$ (**4**) (57% yield) (Scheme 7 (upper)). In this complex, **2a** acted as a *P*,*S*-chelating bidentate ligand. The $^{31}P\{^1H\}$ NMR spectrum of **4** showed a singlet at δ –41.3 ppm. On the other hand, the reaction of $Pd(COD)Cl_2$ with **2a** at a 1:2 molar ratio produced $[PdCl\{Ph_2PC(S)NHPh\text{-}\kappa P,S\}\{Ph_2PC(S)NHPh\text{-}\kappa P\}]Cl$ (**5**) in 77% yield (Scheme 7 (lower)). Although the NH proton signal of **2a** was observed at δ 8.64 ppm in $CDCl_3$, the corresponding signals of **4** and **5** in $CDCl_3$ were observed at δ 13.31 ppm and 13.00 ppm, respectively. These large downfield shifts of the NH proton show the hydrogen

bonding between the NH proton and the Cl atom in solution. The ^{31}P NMR spectra of **5** at various temperatures (20, −10, and −40 °C) are displayed in Figure 4. Coupled two doublets with ^{2}J(PP) = 453.4 Hz were observed at δ –54.2 ppm, 37.8 ppm and those with ^{2}J(PP) = 26.2 Hz were observed at δ –41.9 ppm, 37.3 ppm at 20 °C. We assigned the signals with the largest coupling constant to the *trans* complex and those with the smallest coupling constant to the *cis* complex. The ratio of the *cis* complex increased when the measurement temperature was lowered (*ca.* 1.8:1 at 20 °C, 2.6:1 at −10 °C, and ca. 4.1:1 at −40 °C), and this ratio changed reversibly with the temperature. This behavior has not been reported in previous complexes having phosphinecarbothioamide. Thermodynamic parameters ΔH° (8.6×10^{3} Jmol^{-1}) and ΔS° (2.5×10^{1} JK^{-1} mol^{-1}) of **5** were obtained using van't Hoff plots and were similar to the values found for **3** (see Supplementary Materials, Figure S3).

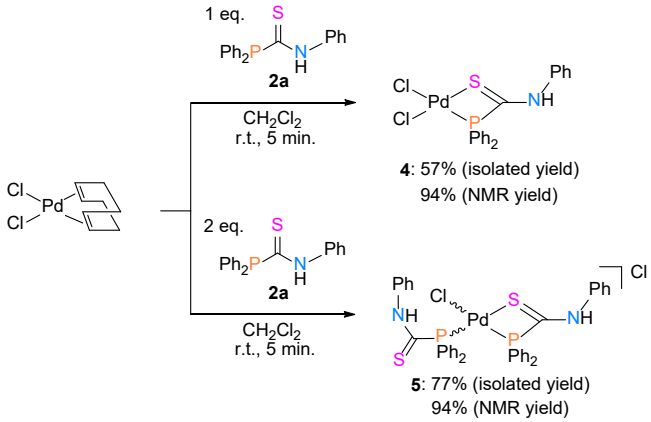

Scheme 7. Reactions of Pd(COD)Cl$_2$ with Ph$_2$PC(S)NHPh **2a**.

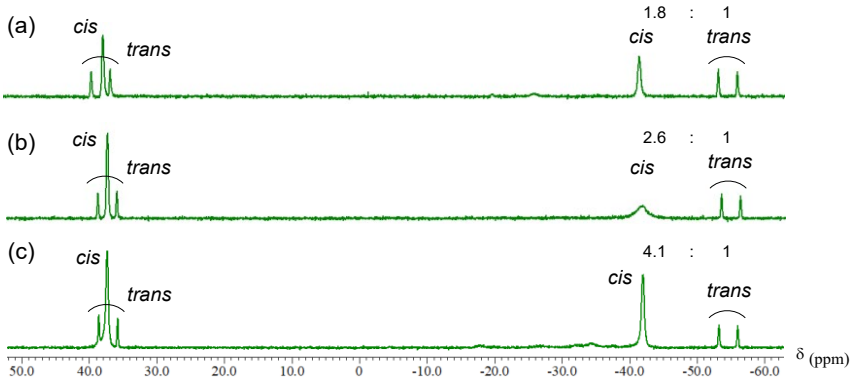

Figure 4. ^{31}P NMR spectra (162 MHz, CD_2Cl_2, ppm) of **5** at 20 °C (**a**), −10 °C (**b**), and −40 °C (**c**).

The structures of **4** and **5** were studied via an X-ray crystal structure analysis. Two independent molecules of **4** crystallized in the unit cell. As these were basically the same, only one molecule (Pd1) is shown in Figure 5a). Complex **4** had a typical square-planar environment; palladium had two Cl atoms situated mutually in *cis* position and *P,S*-coordinated bidentate ligand **2a**. The bond lengths of Pd–P (2.2064(7), 2.1887(7) Å), Pd–S (2.2954(8), 2.2928(8) Å), and Pd–Cl (2.3299(7), 2.3986(7) Å) were similar to those of the previously reported [PdCl$_2${Ph$_2$PC(S)NMe$_2$-κ*P,S*}] complex (2.209(1) Å for Pd–P bond, 2.290(1) Å for Pd–S bond, and 2.329(1), 2.376(1) Å for Pd–Cl bond) [11]. Intermolecular hydrogen bonds between the H1n atoms for the Pd1 molecule and the Cl4 atom for the Pd2 molecule were observed (H1n···Cl4 (2.28(2) Å)). Compound **5** consisted of a cationic palladium complex and a Cl^{-} counter anion (Figure 5b)). In the cationic Pd complex, the Pd atom is coordinated to the phosphorus atom of **2a** as a monodentate ligand, a bidentate *P,S*-bonded **2a**, and a Cl atom, acquiring a square-planar configuration. The two phosphorus atoms were *cis* with respect to each other. This is the first example of a

transition-metal complex with both monodentate and bidentate phosphinecarbothioamide ligands. Complex **5** also showed inter-molecular hydrogen bonds (2.18(3) Å for H1n···Cl2 and 2.29(3) Å for H2n···Cl2) (Figure 6) [25].

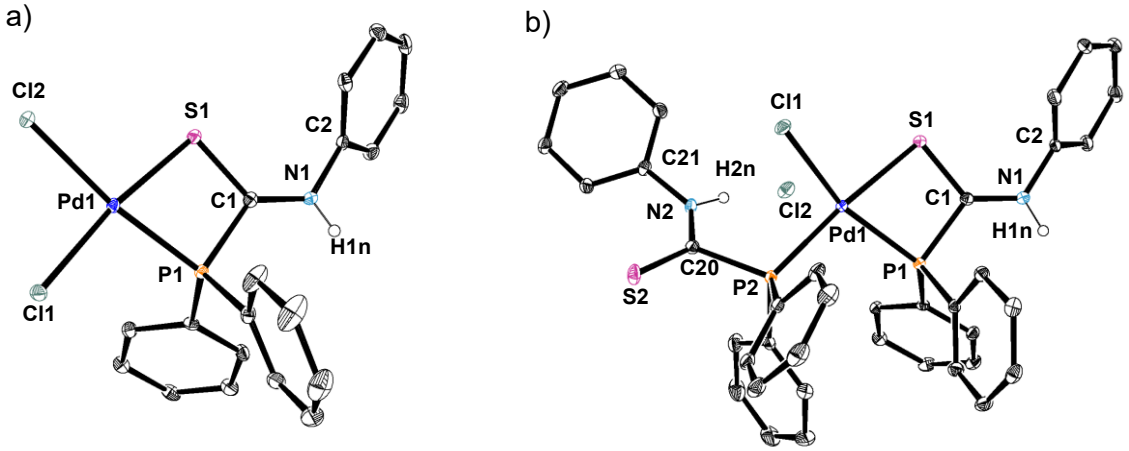

Figure 5. ORTEP drawings of (**a**) **4**·0.5$(CH_3)_2CO$ and (**b**) *cis*-**5**·CH_2Cl_2 with thermal ellipsoids at 30% probability. The crystal solvent and hydrogen atoms (except for NH protons) are omitted for simplicity. Selected bond lengths (Å) and angles (°): Pd1–P1 2.2064(7), Pd1–S1 2.2954(8), Pd1–Cl1 2.3299(7), Pd1–Cl2 2.3534(7), S1–C1 1.704(2), C1–N1 1.302(3), C1–P1 1.844(2), N1–H1n 0.83(2), P1–Pd1–S1 75.47(3), P1–Pd1–Cl1 96.05(3), P1–Pd1–Cl2 171.75(2), S1–Pd1–Cl1 171.48(2), S1–Pd1–Cl2 96.35(3), Cl1–Pd1–Cl2 92.14(3) for **4**; Pd1–P1 2.2324(7), Pd1–P2 2.2886(7), Pd1–S1 2.3448(7), Pd1–Cl1 2.3688(6), S1–C1 1.693(2), C1–N1 1.305(3), C1–P1 1.838(2), N1–H1n 0.89(3), P2–C20 1.876(2), C20–S2 1.651(2), C20–N2 1.324(3), N1–H1n 0.84(3), P1–Pd1–P2 100.41(3), P1–Pd1–S1 74.66(2), P1–Pd1–Cl1 159.01(2), P2–Pd1–S1 174.45(2), P1–C1–S1 103.63(11) for **5**.

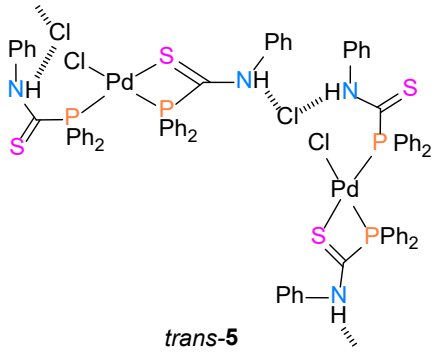

Figure 6. Inter-molecular hydrogen bonds (hash line) for *trans*-**5**.

3. Materials and Methods

3.1. General Considerations

The synthesis of phosphinecarboxamide and phosphinecarbothioamide was carried out using standard Schlenk techniques in a dry nitrogen atmosphere. The synthesis of complexes **3**–**5** was carried out in air. Iron complex $CpFe(CO)_2(Me)$ [34] and palladium complex $PdCl_2(COD)$ [35] were prepared according to the literature method. The other chemicals were commercially available. Phenylphosphine $PhPH_2$ (10% hexane solution) was used after distillation (however, a little amount of hexane could not be removed). Solvents were purified employing a two-column solid-state purification system or were distilled from appropriate drying agents under N_2. Spectroscopic data of the products obtained in this work, **1a**–**1g**, **2a**–**2d, 2f**, and **2k**, agreed with those in the literatures [16,17]. Spectroscopic data of the products **1i**–**1s** were preliminarily reported in [27]. NMR spectra (^1H, ^{13}C, and ^{31}P) were recorded at ambient temperature with a JNM ECS-400 spectrometer.

^{1}H and ^{13}C NMR data were referred to residual peaks of solvent as an internal standard. Peak positions of ^{31}P NMR spectra were referenced to external 85% H_3PO_4 (δ = 140 ppm). Elemental analysis data were obtained with a Perkin–Elmer 2400 CHN elemental analyzer.

3.2. Synthesis

3.2.1. General Procedure for Synthesis of Phosphinecarboxamide and Phosphinecarbothioamide

The mixture of the phosphine compound (0.7 mmol) and isocyanate/isothiocyanate (0.7 mmol) was stirred at room temperature in a Schlenk tube. After the reaction was complete, all volatile materials were removed under reduced pressure. The residual powder was dried in vacuo to give the corresponding phosphinecarboxamide/phosphinecarbothioamide.

m-$ClC_6H_4NHC(O)PPh_2$ (**1h**): Ph_2PH (0.7 mmol, 122 μL) was treated with 3-chlorophenylisocyanate (0.7 mmol, 85 μL) using a general procedure to give the product **1h** (236 mg, 99%) as a white powder. ^{1}H NMR (400 MHz, $CDCl_3$, ppm) δ 7.06–7.07 (m, 1H), 7.16–7.21 (m, 1H), 7.30 (br, 1H), 7.45–7.46 (m, 7H), 7.51–7.53 (m, 1H), 7.57–7.61 (m, 4H). ^{13}C NMR (100.4 MHz, $CDCl_3$, ppm) δ 117.6, 119.7, 124.9, 129.3 (d, $^{3}J_{C\text{-}P}$ = 7.47 Hz), 130.1, 130.4, 132.8 (d, $^{1}J_{C\text{-}P}$ = 10.8 Hz), 134.5 (d, $^{2}J_{C\text{-}P}$ = 19.1 Hz), 134.8, 138.6, 176.6 (d, $^{1}J_{C\text{-}P}$ = 16.6 Hz, C=O). $^{31}P\{^{1}H\}$ NMR (161.70 MHz, $CDCl_3$, ppm) δ –0.76 (s). Elemental analysis (%) calcd for $C_{19}H_{15}ClNOP$: C, 67.17; H, 4.45; N, 4.12. Found: C, 67.20; H, 4.58; N, 3.96%.

p-$CF_3C_6H_4NHC(S)PPh_2$ (**2e**): Ph_2PH (0.7 mmol, 122 μL) was treated with 4-trifluoromethylphenylisothiocyanate (0.7 mmol, 142 mg) using a general procedure to give the product **2e** (270 mg, 99%) as a yellow powder. ^{1}H NMR (400 MHz, $CDCl_3$, ppm) δ 7.45–7.51 (m, 6H), 7.55–7.61 (m, 6H), 7.80 (d, 2H, $^{3}J_{H\text{-}H}$ = 8.8 Hz), 8.78 (br, 1H, NH). ^{13}C NMR (100.4 MHz, $CDCl_3$, ppm) δ 122.1, 126.3 (q, *J* = 3.8 Hz), 129.6 (d, $^{3}J_{C\text{-}P}$ = 6.7 Hz), 130.7, 134.3, 134.5, 134.7, 141.6, 208.5 (d, $^{1}J_{C\text{-}P}$ = 40.3 Hz, C=S). The CF_3 peak overlapped with another peak. ^{19}F NMR (376.95 MHz, $CDCl_3$, ppm) δ 9.20 (s). $^{31}P\{^{1}H\}$ NMR (161.70 MHz, $CDCl_3$, ppm) δ 20.5 (s). Elemental analysis (%) calcd for $C_{20}H_{15}F_3NSP$: C, 61.69; H, 3.88; N, 3.60. Found: C, 61.74; H, 4.00; N, 3.57%.

m-$ClC_6H_4NHC(S)PPh_2$ (**2h**): Ph_2PH (0.7 mmol, 122 μL) was treated with 3-chlorophenylisothiocyanate (0.7 mmol, 92 μL) using a general procedure to give the product **2h** (240 mg, 96%) as a yellow powder. ^{1}H NMR (400 MHz, $CDCl_3$, ppm) δ 7.20–7.22 (m, 1H), 7.26–7.30 (m, 1H), 7.45–7.50 (m, 7H), 7.54–7.58 (m, 4H), 7.74–7.75 (m, 1H), 8.66 (br, 1H, NH). ^{13}C NMR (100.4 MHz, $CDCl_3$, ppm) δ 120.6, 122.4, 127.2, 129.5 (d, $^{3}J_{C\text{-}P}$ = 7.67 Hz), 130.1, 130.6, 134.3, 134.5, 134.5 (d, $^{2}J_{C\text{-}P}$ = 20.3 Hz), 139.8, 207.9 (d, $^{1}J_{C\text{-}P}$ = 40.3 Hz, C= S) ppm. $^{31}P\{^{1}H\}$ NMR (161.70 MHz, $CDCl_3$, ppm) δ 19.4 (s). Elemental analysis (%) calcd for $C_{19}H_{15}ClNSP$: C, 64.14; H, 4.25; N, 3.94 found: C, 63.92; H, 4.33; N, 3.86%.

o-$ClC_6H_4NHC(S)PPh_2$ (**2i**): The mixture of diphenylphosphine Ph_2PH (0.7 mmol, 122 μL) and 2-chlorophenylisothiocyanate (0.7 mmol, 92 μL) was stirred at room temperature in a Schlenk tube. After 24 h, all volatile materials were removed under reduced pressure. The residue was washed with *n*-hexane (1 mL × 3) at −70 °C and dried in vacuo to give **2i** (226 mg, 91%) as a yellow powder. ^{1}H NMR (400 MHz, $CDCl_3$, ppm) δ 7.16 (t, 1H, $^{3}J_{H\text{-}H}$ = 7.8 Hz), 7.28–7.35 (m, 2H), 7.45–7.46 (m, 6H), 7.59–7.62 (m, 4H), 8.95 (d, 1H, $^{3}J_{H\text{-}H}$ = 7.8 Hz), 9.15 (br, 1H, NH). ^{13}C NMR (100.4 MHz, $CDCl_3$, ppm) δ 123.6, 125.8, 127.2, 127.6, 129.5 (d, $^{3}J_{C\text{-}P}$ = 7.47 Hz), 129.7, 130.6, 134.4 (d, $^{1}J_{C\text{-}P}$ = 15.8 Hz), 134.8 (d, $^{2}J_{C\text{-}P}$ = 20.8 Hz), 135.6, 208.2 (d, $^{1}J_{C\text{-}P}$ = 39.9 Hz, C=S). $^{31}P\{^{1}H\}$ NMR (161.70 MHz, $CDCl_3$, ppm) δ 22.2 (s). Elemental analysis (%) calcd for $C_{19}H_{15}ClNSP$: C, 64.14; H, 4.25; N, 3.94. Found: C, 63.97; H, 4.32; N, 3.78%.

$ClC_2H_4NHC(S)PPh_2$ (**2j**): The mixture of Ph_2PH (0.7 mmol, 122 μL) and 2-chloroethylisothiocyanate (0.7 mmol, 68 μL) was stirred at room temperature in a Schlenk tube. After 2 h, all volatile materials were removed under reduced pressure. The residual yellow powder was washed with *n*-hexane (1 mL × 3) at –70 °C and dried in *vacuo* to give **2j** (185 mg, 86%). ^{1}H NMR (400 MHz, $CDCl_3$, ppm) δ 3.53 (t, 2H, *J* = 9.2 Hz, CH_2), 4.58–4.63 (m, 2H, CH_2), 7.46–7.55 (m, 6H), 7.58–7.62 (m, 4H). The peak of NH overlapped with another peak. ^{13}C NMR (100.4 MHz, $CDCl_3$, ppm) δ 32.2, 58.0, 129.6 (d, $^{3}J_{C\text{-}P}$ = 8.3 Hz,

m-Ph), 131.7, 134.6, 134.9, 202.2 (d, $^{1}J_{C\text{-}P}$ = 59.0 Hz, C=S). $^{31}P\{^{1}H\}$ NMR (161.70 MHz, $CDCl_3$, ppm) δ –4.20 (s). Elemental analysis (%) calcd for $C_{15}H_{15}ClNSP$: C, 58.54; H, 4.91; N, 4.55. Found: C, 57.99; H, 4.97; N, 4.44%.

3.2.2. NMR Tube Experiments for Pd(II) Complexes

A $CDCl_3$ solution (0.5 mL) of $Pd(COD)Cl_2$ (5.8 mg, 0.020 mmol), $Ph_2PC(O)NHPh$ **1a** (6.2 mg, 0.020 mmol) and $P(=O)Ph_3$ (internal standard, 5.3 mg, 0.019 mmol) was mixed in an NMR tube at room temperature. After 5 minutes, ^{31}P NMR was measured, which revealed that [Pd{$Ph_2PC(O)NHPh$-κ*P*}$_2Cl_2$] (**3**) was formed in 48% NMR yield based on Pd.

A $CDCl_3$ solution (0.5 mL) of $Pd(COD)Cl_2$ (7.1 mg, 0.025 mmol), $Ph_2PC(S)NHPh$ **2a** (8.1 mg, 0.025 mmol) and $P(=O)Ph_3$ (internal standard, 8.1 mg, 0.029 mmol) was mixed in an NMR tube at room temperature. After 5 minutes, ^{31}P NMR was measured, which revealed that [$PdCl_2${$Ph_2PC(S)NHPh$-κ*P,S*}] (**4**) was formed in 94% NMR yield.

A $CDCl_3$ solution (0.5 mL) of $Pd(COD)Cl_2$ (7.1 mg, 0.025 mmol), $Ph_2PC(S)NHPh$ **2a** (16.1 mg, 0.050 mmol), and $P(=O)Ph_3$ (internal standard, 8.1 mg, 0.029 mmol) was mixed in an NMR tube at room temperature. After 5 minutes, ^{31}P NMR was measured, which revealed that [PdCl{$Ph_2PC(S)NHPh$-κ*P,S*}{(*P*-)$Ph_2PC(S)NHPh$}]Cl (**5**) was formed in 94% NMR yield.

3.2.3. Synthesis of Pd(II) Complexes

[Pd{$Ph_2PC(O)NHPh$-κ*P*}$_2Cl_2$] (**3**): A dichloromethane solution (2.5 mL) in a flask containing $PdCl_2(COD)$ (57.2 mg, 0.20 mmol) and $Ph_2PC(O)NHPh$ **1a** (122.3 mg, 0.40 mmol) was stirred at room temperature. After 5 min, all volatile materials were removed under reduced pressure. The residual yellow powder was washed with *n*-hexane and dried in vacuo to give **3** (153.7 mg, 0.195 mmol, 97%) as a yellow powder. ^{1}H NMR (400 MHz, $CDCl_3$, ppm) δ 7.11–7.16 (m, 2H), 7.28–7.30 (m, 4H), 7.46–7.50 (m, 8H), 7.54–7.59 (m, 8H), 7.81–7.86 (m, 8H), 10.56 (br, 2H, NH). $^{13}C\{^{1}H\}$ NMR (100.4 MHz, $CDCl_3$, ppm) δ 120.3 (s), 125.6 (s), 126.3 (vt, $J_{C\text{-}P}$ = 24.9 Hz), 128.7 (vt, *J* = 5.3 Hz), 129.2 (s), 131.8 (s), 135.0 (vt, *J* = 6.2 Hz), 137.6 (vt, *J* = 4.8 Hz), 164.9 (vt, *J* = 26.4 Hz, C=O). $^{31}P\{^{1}H\}$ NMR (162 MHz, $CDCl_3$, ppm) δ 25.5 (s). Elemental analysis (%) calcd for $C_{38}H_{32}Cl_2N_2O_2P_2Pd$: C, 57.92; H, 4.09; N, 3.56. Found: C, 57.66; H, 4.22; N, 3.50%.

[$PdCl_2${$Ph_2PC(S)NHPh$-κ*P,S*}] (**4**): A dichloromethane solution (1.0 mL) in a test tube containing $PdCl_2(COD)$ (14.3 mg, 0.050 mmol) and $Ph_2PC(S)NHPh$ **2a** (32.2 mg, 0.100 mmol) was stirred at room temperature for 5 min. Yellow crystal **4** (14.3 mg, 0.029 mmol, 57%) was obtained by solvent diffusion over a few days from a CH_2Cl_2 layer and an overlayer of hexane. ^{1}H NMR (400 MHz, −50 °C, $CDCl_3$, ppm) δ 7.36–7.53 (m, 10H), 7.88–7.90 (m, 2H), 7.99–8.04 (m, 3H), 13.31 (brs, NH, 1H). $^{13}C\{^{1}H\}$ NMR (100.4 MHz, 20 °C, $CDCl_3$, ppm) δ 119.8 (s), 120.3 (s), 123.7 (s), 129.6 (s), 129.9 (d, $J_{C\text{-}P}$ = 12.5 Hz), 134.0 (s), 135.0 (d, $J_{C\text{-}P}$ = 13.4 Hz), 135.5 (d, $J_{C\text{-}P}$ = 4.8 Hz), The C=S peak was not observed. $^{31}P\{^{1}H\}$ NMR (162 MHz, 20 °C, $CDCl_3$, ppm) δ −41.3 (s). Elemental analysis (%) calcd for $C_{19}H_{16}Cl_2NPPdS$: C, 45.76; H, 3.23; N, 2.81. Found: C, 45.97; H, 3.57; N, 2.76%.

[PdCl{$Ph_2PC(S)NHPh$-κ*P,S*}{(*P*-)$Ph_2PC(S)NHPh$}]Cl (**5**). A dichloromethane solution (1.0 mL) in a test tube containing $PdCl_2(COD)$ (14.3 mg, 0.050 mmol) and $Ph_2PC(S)NHPh$ **2a** (32.2 mg, 0.10 mmol) was stirred at room temperature for 5 min. The orange powder **5** (35.0 mg, 0.039 mmol, 77%) was obtained via solvent diffusion over a few days from a CH_2Cl_2 layer and an overlayer of hexane. ^{1}H NMR (400 MHz, –40 °C, CD_2Cl_2, ppm) δ 6.08 (brs, NH, 1H), 7.14–7.18 (m, 8H), 7.35–7.43 (m, 19H), 8.09–8.11 (m, 3H), 13.0 (brs, NH, 1H). $^{31}P\{^{1}H\}$ NMR (162 MHz, –40 °C, CD_2Cl_2, ppm) δ 37.8 (d, *J* = 453.4 Hz, *trans*), 37.3 (d, *J* = 26.2 Hz, *cis*), –41.9 (d, *J* = 26.2 Hz, *cis*), –54.2 (d, *J* = 453.4 Hz, *trans*). Elemental analysis (%) calcd for $C_{38}H_{32}Cl_2N_2P_2PdS_2$: C, 55.66; H, 3.93; N, 3.42. Found: C, 55.99; H, 4.30; N, 3.33%.

3.3. Crystallography

Crystallographic data are summarized in Table 1. The single crystals of **1i**, **2c**, and **3**–**5** were obtained using the slow diffusion method (CH_2Cl_2/hexane for **3** and **5**; acetone/ether for **4**). Diffraction-intensity data were collected with Rigaku AFC11 with a Saturn 724 + CCD diffractometer (200(2) K for **1i**, **2c**; 110(2) K for **3**–**5**), and semiempirical multi-scan absorption correction [36] was performed. The structures were solved using SIR97 [37] via subsequent difference Fourier synthesis, and refined with full matrix least-squares procedures on F^2. All non-hydrogen atoms were refined with anisotropic displacement coefficients. NH protons were determined via difference Fourier synthesis and refined isotropically. Hydrogen atoms (except for NH protons) were treated as idealized contributions and refined in a rigid group model. All software and sources of scattering factors were contained in the SHELXL-2018/3 [38] program package. The Cambridge Crystallographic Data Centre (CCDC) deposition numbers of **1i**, **2c**, and **3**–**5** are included in Table 1.

Table 1. Crystallographic data and details of structure refinement parameters of **1i**, **2c**, and **3**–**5**

	1i	**2c**	**3**	**4**·**0.5(CH$_3$)$_2$CO**	**5**·**CH$_2$Cl$_2$**
empirical formula	$C_{15}H_{15}ClNOP$	$C_{19}H_{15}ClNPS$	$C_{38}H_{32}Cl_2N_2O_2P_2Pd$	$C_{20.5}H_{19}Cl_2NO_{0.5}PSPd$	$C_{39}H_{34}Cl_4N_2P_2S_2Pd$
formula weight	291.70	355.80	787.89	527.70	904.94
T (K)	200(2)	200(2)	110(2)	110(2)	110(2)
crystal system	triclinic	monoclinic	orthorhombic	triclinic	monoclinic
space group	$P\bar{1}$	$P2_1/n$	$Pca2_1$	$P\bar{1}$	$P2_1/n$
a (Å)	9.29470(10)	9.2578(5)	12.9390(2)	9.679(3)	17.288(5)
b (Å)	11.8190(2)	21.2798(9)	12.4521(3)	14.927(4)	13.508(3)
c (Å)	21.0466(4)	9.9399(5)	21.0466(4)	15.962(4)	18.189(5)
α (°)	85.569(6)			106.543(4)	
β (°)	82.125(7)	116.3332(15)		92.7607(7)	112.506(3)
γ (°)	67.021(6)			103.748(3)	
volume (Å^3)	1448.16(9)	1755.00(15)	3390.98(12)	2130.6(10)	3924.0(17)
Z	4	4	4	4	4
ρ_{calcd} (mg m^{-3})	1.338	1.347	1.543	1.645	1.532
μ (mm^{-1})	0.365	0.426	0.837	1.303	0.965
F(000)	608	736	1600	1056	1832
crystal size (mm^3)	0.37 × 0.27 × 0.12	0.27 × 0.18 × 0.17	0.12 × 0.07 × 0.02	0.13 × 0.07 × 0.03	0.21 × 0.16 × 0.06
reflections collected	17,154	13,335	27,555	22,263	39,512
R(int)	6564 (0.0361)	3974 (0.0253)	5973 (0.0309)	9665 (0.0288)	8955 (0.0336)
$R1$ ($I > 2\sigma(I)$)	0.0478	0.0503	0.0204	0.0278	0.0346
w$R2$ (all data)	0.1187	0.1062	0.0502	0.0600	0.0704
goodness of fit	1.106	1.094	1.042	1.046	1.094
CCDC deposition number	1959302	2193371	2168755	2168782	2168783

4. Conclusions

We achieved the catalyst-free synthesis of phosphinecarboxamide and phosphinecarbothioamide through the hydrophosphination of isocyanates and isothiocyanates. The important point in our system was to carry out the reaction without using a solvent (neat). This system showed the characteristics of easy handling, high yield, short reaction time, and good functional-group tolerance for the functionalized isocyanates and isothiocyanates. For the requirement of no catalyst nor solvent, the gram-scale synthesis of these compounds was also achieved. In addition, we synthesized and characterized palladium complexes with phosphinecarboxamide and phosphinecarbothioamide as ligands. In the reaction of $Pd(COD)Cl_2$ with **1a**, [Pd{$Ph_2PC(O)NHPh$-κP}$_2Cl_2$] (**3**) was obtained regardless of whether **1a** was used in 1 or 2 equivalents. In contrast, in the reaction of $Pd(COD)Cl_2$ with **2a**, [$PdCl_2${$Ph_2PC(S)NHPh$-κP,S}] (**4**) and [PdCl{$Ph_2PC(S)NHPh$-κP,S}{$Ph_2PC(S)NHPh$-κP}]Cl (**5**) were selectively obtained when 1 eq. and 2 eq. of **2a** were used, respectively. It was revealed that **3** and **5** having intra- and/or inter-molecular hydrogen bonds showed thermal *cis/trans* isomerization.

Supplementary Materials: The following supporting information can be downloaded at: https://www.mdpi.com/xxx/s1, Figure S1: ^{31}P NMR spectra ($CDCl_3$, 161.70 MHz) of **3** at 50 °C, 20 °C, and −50 °C, Figure S2: van't Hoff plots for **3**, Figure S3: van't Hoff plots for **5**, Figures S4–S27: NMR spectra of all new compounds.

Author Contributions: M.I., T.M. (Toshiyuki Moriuchi) and H.N. conceived, designed, and wrote the paper. K.O., T.M. (Takanari Matsutani) and T.N. performed experiments and analyzed the data. All authors have read and agreed to the published version of the manuscript.

Funding: This research received no external funding.

Institutional Review Board Statement: Not applicable.

Informed Consent Statement: Not applicable.

Data Availability Statement: The crystallographic data are available from the Cambridge Crystallographic Data Centre (CCDC). Other data not presented in Supplementary Materials are available upon request from the corresponding author.

Acknowledgments: We thank R. Tanaka, Osaka Metropolitan University, for single-crystal X-ray structure analysis. Thanks are also due to the Analytical Centre, Graduate School of Science, Osaka Metropolitan University.

Conflicts of Interest: The authors declare no conflict of interest.

Sample Availability: Samples of the compounds are not available from the authors.

References

1. Geeson, M.B.; Jupp, A.R.; McGrady, J.E.; Goicoechea, J.M. On the coordination chemistry of phosphinecarboxamide: Assessing ligand basicity. *Chem. Commun.* **2014**, *50*, 12281–12284. [CrossRef] [PubMed]
2. Bennett, J.; Doyle, R.J.; Lee, H.-Y.; Lu, D.; Salem, G.; Speldewinde, D.J.; Tifan, M.; Willis, A.C. Synthesis of 1,3-azaphosphol-2-ones. Crystal and molecular structures of [*SP-4-2*]-dichlorobis(3-phenyl-1,3-dihydrobenzo [1,3]azaphosphol-2-one-P)palladium(II) and its chloro(methyl)platinum(II) analogue. *Dalton Trans.* **2010**, *39*, 256–264. [CrossRef] [PubMed]
3. Jupp, A.R.; Trott, G.; de la Garanderie, É.P.; Holl, J.D.G.; Carmichael, D.; Goicoechea, J.M. Exploiting the brønsted acidity of phosphinecarboxamides for the synthesis of new phosphides and phosphines. *Chem. Eur. J.* **2015**, *21*, 8015–8018. [CrossRef] [PubMed]
4. Navrátil, M.; Faria, E.N.; Panahy, G.; Císařová, I.; Goicoechea, J.M.; Štěpnička, P. Novel ferrocenyl functionalised phosphinecarboxamides: Synthesis, characterisation and coordination. *Dalton Trans.* **2020**, *49*, 8645–8651. [CrossRef]
5. Cowan, S.W.; Dakternieks, D.; Gable, R.W.; Hoskins, B.F.; Rolls, C.L.; Tiekink, E.R.T. Studies of some cadmium(II) and mercury(II) complexes with dicyclohexylphosphino-*N*-phenylthioformamide, LH: Crystal and molecular-structures of $[CdI_2(LH)]_2$, $([HgCl_2(LH)]_2.CH_2Cl_2)$ and $HgCl_2(LH)_2$. *Aust. J. Chem.* **1986**, *39*, 547–556. [CrossRef]
6. Malisch, W.; Spörl, A.; Thirase, K.; Fey, O. Übergangsmetall-substituierte phosphane, arsane und stibane, LIX [1], ein addukt des Me_3P-substituierten ferrio-diphenylphosphans $Cp(OC)(Me_3P)Fe\text{-}PPh_2$ mit methylisothiocyanat: Darstellung, protonierung und methylierung. *Z. Naturforsch.* **1998**, *53*, 1077–1083. [CrossRef]
7. Crespo, O.; Fernández, E.J.; Jones, P.G.; Laguna, A.; López-de-Luzuriaga, J.M.; Monge, M.; Olmos, M.E.; Pérez, J. Coordination modes of diphenylphosphinothioformamide in its neutral and deprotonated forms at gold(I). *Dalton Trans.* **2003**, 1076–1082. [CrossRef]
8. Just, B.; Klein, W.; Kope, J.; Steinhäuser, K.G.; Kramolowsky, R. Synthese und koordinationsverhalten ambidenter chelatliganden: III. Kristall-und molekülstrukturen der carbonyl-mangan(I)-komplexe *fac*-$[MnBr(CO)_3\{Ph_2PC(S)NPhH\}]$ und $[Mn\{S(NPh)CPPh_2\}(CO)_4]$. Neutrale phosphinothioformamide und deren deprotonierte, anionische derivate als *S,P*-chelatliganden. *J. Organomet. Chem.* **1982**, *229*, 49–61.
9. Kunze, U.; Jawad, H.; Hiller, W.; Naumer, R. Phosphinsubstituierte chelatliganden, XIV [1] wasserstoff-brückenbindung in THF-addukten von tetracarbonylchrom- und -molybdänkomplexen mit P,S-koordinierten phosphinothioformamid-liganden. Kristallstruktur von $[(CO)_4Cr(PPh_2C(S)NHMe)]\cdot THF$. *Z. Naturforsch.* **1985**, *40*, 512–517.
10. Siasios, G.; Tiekink, E.R.T. Synthesis and crystal structure of $[Ni\{Ph_2PC(S)NPh\}_2]$ and $[Ni\{Ph_2P(Y)C(S)NPh\}_2]$(Y = S or Se). *J. Chem. Soc. Dalton Trans.* **1996**, 2269–2273. [CrossRef]
11. Leung, P.-H.; Qin, Y.; He, G.; Mok, K.F.; Vittal, J.J. Coordination chemistry, reactivities, and stereoelectronic properties of chelating phosphine ligands containing thioamide substituents. *J. Chem. Soc., Dalton Trans.* **2001**, *3*, 309–314. [CrossRef]
12. Ambrosius, H.P.M.M.; Willemse, J.; Cras, J.A.; Bosman, W.P.; Noordik, J.H. Different coordination modes of neutral and deprotonated ZC(S)N(H)R ligands (Z = PPh_2, R = Ph, Me; Z = NMe_2, R = Ph) in molybdenum and tungsten complexes. X-ray structure analysis of $[Mo(CO)_2[Ph_2PC(S)NMe][\mu\text{-}Ph_2PC(S)NMe]]_2\cdot CH_2Cl_2$. *Inorg. Chem.* **1984**, *23*, 2672–2678. [CrossRef]

13. Kunze, U.; Jawad, H.; Burghardt, R. Phosphinsubstituierte chelatliganden, XX [1] darstellung und diastereoselektive komplexierung von chiralen phosphinothioformamiden, $Ph_2P(X)C(S)NHCHMePh$ (X = 2 e^-, O, S). *Z. Naturforsch.* **1986**, *41*, 1142–1150.
14. Ambrosius, H.P.M.M.; Cotton, F.A.; Falvello, L.R.; Hintzenl, H.T.J.M.; Melton, T.J.; Schwotzer, W.; Tomas, M.; van der Linden, J.G.M. Formation of isomeric dimolybdenum(II) compounds using the potentially ambidentate ligands $[R_2PC(S)NR']^-$ (R/R′ = Ph/Ph, Ph/Me) and $[Me_2NC(S)NPh]^-$. *Inorg. Chem.* **1984**, *23*, 1611. [CrossRef]
15. Buckler, S.A. Reaction of phosphine with Isocyanates. *J. Org. Chem.* **1959**, *24*, 1460–1462. [CrossRef]
16. Behrle, A.C.; Schmidt, J.A.R. Insertion eeactions and catalytic hydrophosphination of heterocumulenes using α-metalated *N,N*-dimethylbenzylamine rare-earth-metal complexes. *Organometallics* **2013**, *32*, 1141–1149. [CrossRef]
17. Gu, X.; Zhang, L.; Zhu, X.; Wang, S.; Zhou, S.; Wei, Y.; Zhang, G.; Mu, X.; Huang, Z.; Hong, D.; et al. Synthesis of bis(NHC)-based CNC-pincer rare-earth-metal amido complexes and their application for the hydrophosphination of heterocumulenes. *Organometallics* **2015**, *34*, 4553–4559. [CrossRef]
18. Karmel, I.S.; Tamm, M.; Eisen, M.S. Actinide-mediated catalytic addition of E–H bonds (E=N, P, S) to carbodiimides, isocyanates, and isothiocyanates. *Angew. Chem. Int. Ed.* **2015**, *54*, 12422–12425. [CrossRef]
19. Batrice, R.J.; Eisen, M.S. Catalytic insertion of E–H bonds (E = C, N, P, S) into heterocumulenes by amido-actinide complexes. *Chem. Sci.* **2016**, *7*, 939–944. [CrossRef]
20. Sharpe, H.R.; Geer, A.M.; Lewis, W.; Blake, A.J.; Kays, D.L. Iron(II)-catalyzed hydrophosphination of isocyanates. *Angew. Chem. Int. Ed.* **2017**, *56*, 4845–4848. [CrossRef]
21. Zhang, B.; Ma, X.; Yan, B.; Ni, C.; Yu, H.; Yang, Z.; Roesky, H.W. An efficient catalytic method for hydrophosphination of heterocumulenes with diethylzinc as precatalyst without a solvent. *Dalton Trans.* **2021**, *50*, 15488–15492. [CrossRef]
22. Zhang, Y.; Qu, L.; Wang, Y.; Yuan, D.; Yao, Y.; Shen, Q. Neutral and cationic zirconium complexes bearing multidentate aminophenolato ligands for hydrophosphination reactions of alkenes and heterocumulenes. *Inorg. Chem.* **2018**, *57*, 139–149. [CrossRef] [PubMed]
23. Downie, T.M.H.; Hall, J.W.; Finn, T.P.C.; Liptrot, D.J.; Lowe, J.P.; Mahon, M.F.; McMullin, C.L.; Whittlesey, M.K. The first ring-expanded NHC-copper(I) phosphides as catalysts in the highly selective hydrophosphination of isocyanates. *Chem. Commun.* **2020**, *56*, 13359–13362. [CrossRef] [PubMed]
24. Schwamm, R.J.; Coles, M.P. Catalytic hydrophosphination of isocyanates by molecular antimony phosphanides. *Eur. J. Inorg. Chem.* **2022**, *2022*, e202200064. [CrossRef]
25. Ito, M.; Iseki, M.; Itazaki, M.; Nakazawa, H. Tetrahedral cage complex with planar vertices: Selective synthesis of Pt_4L_6 cage complexes involving hydrogen bonds driven by halide binding. *Chem. Commun.* **2016**, *52*, 7205–7208.
26. Matsutani, T.; Itazaki, M.; Akine, S.; Moriuchi, T. Macrocyclic dimer of $Fc(NHC(O)PPh_2\text{-}AuCl)_2$ induced by aurophilic interactions, and chirality induction into Fc core. *J. Organomet. Chem.* **2020**, *912*, 121182.
27. Itazaki, M.; Matsutani, T.; Nochida, T.; Moriuchi, T.; Nakazawa, H. Convenient synthesis of phosphinecarboxamide and phosphinecarbothioamide by hydrophosphination of isocyanates and isothiocyanates. *Chem. Commun.* **2020**, *56*, 443–445. [CrossRef]
28. Kamitani, M.; Itazaki, M.; Tamiya, C.; Nakazawa, H. Regioselective double hydrophosphination of terminal arylacetylenes catalyzed by an iron complex. *J. Am. Chem. Soc.* **2012**, *134*, 11932–11935. [CrossRef]
29. Itazaki, M.; Katsube, S.; Kamitani, M.; Nakazawa, H. Synthesis of vinylphosphines and unsymmetric diphosphines: Iron-catalyzed selective hydrophosphination reaction of alkynes and vinylphosphines with secondary phosphines. *Chem. Commun.* **2016**, *52*, 3163–3166. [CrossRef]
30. Zhu, X.; Xu, M.; Sun, J.; Guo, D.; Zhang, Y.; Zhou, S.; Wang, S. Hydroamination and hydrophosphination of isocyanates/isothiocyanates under catalyst-free conditions. *Eur. J. Org. Chem.* **2021**, 5213–5218. [CrossRef]
31. Jupp, A.R.; Goicoechea, J.M. Phosphinecarboxamide: A phosphorus-containing analogue of urea and stable primary phosphine. *J. Am. Chem. Soc.* **2013**, *135*, 19131–19134. [CrossRef] [PubMed]
32. Redfield, D.A.; Nelson, J.H. Equilibrium energetics of cis-trans isomerization for two square-planar palladium(II)-phosphine complexes. *Inorg. Chem.* **1973**, *12*, 15–19. [CrossRef]
33. Redfield, D.A.; Cary, L.W.; Nelson, J.H. Equilibrium thermodynamics and mechanism of cis-trans isomerization for diazidobis(methyldiphenylphosphine)palladium(II) and diazidobis(dimethylphenylphosphine)palladium(II). *Inorg. Chem.* **1975**, *14*, 50–59. [CrossRef]
34. Piper, T.S.; Wilkinson, G. Alkyl and aryl derivatives of π-cyclopentadienyl compounds of chromium, molybdenum, tungsten, and iron. *J. Inorg. Nucl. Chem.* **1956**, *3*, 104–124. [CrossRef]
35. Drew, D.; Doyle, J.R. Cyclic diolefin complexes of platinum and palladium. *Inorg. Synth.* **1972**, *13*, 47–55.
36. Rigaku. *REQAB*; Version 1.1; Rigaku Corporation: Tokyo, Japan, 1998.
37. Altomare, A.; Burla, M.C.; Camalli, M.; Cascarano, G.; Giacovazzo, C.; Guagliard, A.; Moliterni, A.G.G.; Spagna, R. SIR97: A new tool for crystal structure determination and refinement. *J. Appl. Crystallogr.* **1999**, *32*, 115–119. [CrossRef]
38. Sheldrick, G.M. Crystal structure refinement with SHELXL. *Acta Crystallogr.* **2015**, *71*, 3–8.